Interferon Resistance of Emerging SARS-CoV-2 Variants

Kejun Guo[1], Bradley S. Barrett[1], Kaylee L. Mickens[1,2], Ezster K. Vladar[3], James H. Morrison[1], Kim J. Hasenkrug[4], Eric M. Poeschla[1], and Mario L. Santiago[1,2]*

[1]*Division of Infectious Diseases, Department of Medicine, University of Colorado Anschutz Medical Campus, Aurora, CO, USA 80045*

[2]*Department of Immunology and Microbiology, University of Colorado Anschutz Medical Campus, Aurora, CO, USA 80045*

[3]*Division of Pulmonary Sciences and Critical Medicine, Department of Medicine, University of Colorado Anschutz Medical Campus, Aurora, CO, USA 80045*

[4]*Rocky Mountain Laboratories, National Institutes of Allergy and Infectious Diseases, National Institutes of Health, Hamilton, MT 59840*

*To whom correspondence should be addressed: mario.santiago@ucdenver.edu

Abstract

The emergence of SARS-CoV-2 variants with enhanced transmissibility, pathogenesis and resistance to vaccines presents urgent challenges for curbing the COVID-19 pandemic. While Spike mutations that enhance virus infectivity or neutralizing antibody evasion may drive the emergence of these novel variants, studies documenting a critical role for interferon responses in the early control of SARS-CoV-2 infection, combined with the presence of viral genes that limit these responses, suggest that interferons may also influence SARS-CoV-2 evolution. Here, we compared the potency of 17 different human interferons against multiple viral lineages sampled during the course of the global outbreak, including ancestral and four major variants of concern. Our data reveal increased interferon resistance in emerging SARS-CoV-2 variants, suggesting that evasion of innate immunity may be a significant, ongoing driving force for SARS-CoV-2 evolution. These findings have implications for the increased lethality of emerging variants and highlight the interferon subtypes that may be most successful in the treatment of early infections.

Author Summary

In less than 2 years since its spillover into humans, SARS-CoV-2 has infected over 220 million people, causing over 4.5 million COVID-19 deaths. High infection rates provided substantial opportunities for the virus to evolve, as variants with enhanced transmissibility, pathogenesis, and resistance to vaccine-elicited neutralizing antibodies have emerged. While much focus has centered on the Spike protein which the virus uses to infect target cells, mutations were also found in other viral proteins that might inhibit innate immune responses. Specifically, viruses encounter a potent innate immune response mediated by the interferons, two of which, IFNα2 and IFNβ, are being repurposed for COVID-19 treatment. Here, we compared the potency of

human interferons against ancestral and emerging variants of SARS-CoV-2. Our data revealed increased interferon resistance in emerging SARS-CoV-2 strains that included the alpha, beta, gamma and delta variants of concern, suggesting a significant, but underappreciated role for innate immunity in driving the next phase of the COVID-19 pandemic.

Results

The human genome encodes a diverse array of antiviral interferons (IFNs). These include the type I IFNs (IFN-Is) such as the 12 IFNα subtypes, IFNβ and IFNω that signal through ubiquitous IFNAR receptor, and the type III IFNs (IFN-IIIs) such as IFNλ1, IFNλ2 and IFNλ3 that signal through the more restricted IFNλR receptor that is present in lung epithelial cells [1]. IFN diversity may be driven by an evolutionary arms-race in which viral pathogens and hosts reciprocally evolve countermeasures [2]. For instance, the IFNα subtypes exhibit >78% amino acid sequence identity, but IFNα14, IFNα8 and IFNα6 most potently inhibited HIV-1 *in vitro* and *in vivo* [3-5], whereas IFNα5 most potently inhibited influenza H3N2 in lung explant cultures [6]. Even though SARS-CoV-2 was sensitive to IFNα2, IFNβ, and IFNλ [7-9], and clinical trials of IFNα2 and IFNβ demonstrated therapeutic promise for COVID-19 [10-12], a direct comparison of multiple IFN-Is and IFN-IIIs against diverse SARS-CoV-2 variants of concern has not yet been done.

The current study was initially undertaken to determine which IFNs would best inhibit SARS-CoV-2. These first set of experiments were performed between December 2020 and March 2021, and we selected 5 isolates from prominent lineages [13] during this phase of the pandemic (Fig 1, S1 Table). USA-WA1/2020 is the standard strain utilized in many *in vitro* and *in vivo* studies of SARS-CoV-2 and belongs to lineage A [13]. It was isolated from the first COVID-19 patient in the US, who had a direct epidemiologic link to Wuhan, China, where the virus was first detected [14]. By contrast, subsequent infection waves from Asia to Europe [15] were associated with the emergence of the D614G mutation [16]. Lineage B strains with G614 spread globally and displaced ancestral viruses with striking speed, likely due to increased transmissibility [17,

18]. These strains accumulated additional mutations in Italy as lineage B.1 which then precipitated a severe outbreak in New York City [19]. Later in the United Kingdom (U.K.), lineage B.1.1.7 acquired an N501Y mutation associated with enhanced transmissibility [13]. Lineage B.1.351, first reported in South Africa, additionally acquired an additional E484K mutation associated with resistance to neutralizing antibodies [20, 21]. Both B.1.1.7 and B.1.351 were reported in multiple countries and in some cases have become dominant for extended periods [22]. We obtained representative SARS-CoV-2 isolates of the B, B.1, B.1.1.7 and B.1.351 lineages (S1 Table). Each stock was sourced from beiresources.org and amplified once in a human alveolar type II epithelial cell line (A549) that we have stably transduced with the receptor ACE2 (A549-ACE2) (S1A Fig).

A549-ACE2 cells were pre-incubated with 17 recombinant IFNs (PBL Assay Science) overnight in parallel and in triplicate, then infected with a non-saturating virus dose for 2 h (S1B Fig). We normalized the IFNs based on molar concentrations similarly to our previous work with HIV-1 [3, 23]. To enable high-throughput evaluation of the antiviral activities of the numerous IFNs against the multiple live SARS-CoV-2 isolates, we used a quantitative PCR (qPCR) assay to determine amounts of virus produced 24 hours after infection (Fig 2A). Initial dose-titrations showed that a 2 pM concentration fell within the dynamic range of activity and maximally distinguished the antiviral activities of IFNs with widely divergent potencies, i.e., IFNβ and IFNλ1 (S1C Fig). Of note, the IFNβ and IFNλ1 doses used did not significantly affect cell viability (S1D Fig). Thus, 2 pM doses were used for additional antiviral activity testing. We also evaluated the qPCR assay against a VeroE6 plaque assay using triplicate serial dilutions of a SARS-CoV-2 isolate (B.1.351). Virus titers obtained using these two assays were strongly

correlated (S2A Fig). However, the VeroE6 plaque assay had ~2-log lower dynamic range; we estimate that 1 plaque forming unit corresponds to ~900 SARS-CoV-2 N1 copies (S2A Fig). Virus copy numbers also correlated with the numbers of primary airway epithelial cells infected with different SARS-CoV-2 variants as quantified by immunofluorescence (S2B Fig). Thus, we employed the qPCR assay to robustly distinguish the antiviral activity of the different interferons.

In the absence of IFN, all 5 isolates reached titers of ~10^4-10^6 copies per 5 µl input of RNA extract (Fig 2). Using absolute copy numbers (Fig 2) or values normalized to mock as 100% (S2 Fig), the 17 IFNs showed a range of antiviral activities against SARS-CoV-2. The 3 IFNλ subtypes exhibited none to very weak (<2-fold) antiviral activities compared to most IFN-Is (Fig 2 and S3 Fig, blue bars). This was despite the fact that the assay showed a robust dynamic range, with some IFNs inhibiting USA-WA1/2020 >2500-fold to below detectable levels (Fig 2A). IFN potencies against the 5 isolates correlated with each other (S4 Fig), and a similar rank-order of IFN antiviral potency was observed for G614+ isolates (Fig 2B, S3 Fig). Overall, IFNα8, IFNβ and IFNω were the most potent, followed by IFNα5, IFNα17 and IFNα14 (Fig 2C); the type III (λ) IFNs were least potent.

The molecular basis for the diverse antiviral effects of the highly related IFNα subtypes has been an active area of investigation, particularly with regard to the relative contributions of quantitative (signaling) versus qualitative (differential gene regulation) mechanisms [2-5]. We reported that inhibition of HIV-1 by the IFNα subtypes correlated with IFNAR signaling capacity and binding affinity to the IFNAR2 subunit [3, 23]. IFNAR signaling capacity, as

measured in an IFN-sensitive reporter cell line (iLite cells; Euro Diagnostics), correlated with the antiviral potencies of the IFNα subtypes against SARS-CoV-2 lineages A and B, but not B.1, B.1.351 or B.1.1.7 (Fig 3A). IFNAR binding affinities as measured by surface plasmon resonance by the Schreiber group [24] did not correlate with IFNα subtype inhibition of SARS-CoV-2 (Fig 3B). As the recombinant IFNs used in this study was from the same source as that of the prior HIV-1 study [3, 23], we also determined if the IFNs that potently inhibit HIV-1 also function similarly against SARS-CoV-2. Notably, the correlations between SARS-CoV-2 and HIV-1 inhibition [3] were weak at best (Fig 3C). These findings suggested that IFN-mediated control of SARS-CoV-2 isolates may be qualitatively distinct from that of HIV-1.

We generated a heat-map to visualize the antiviral potency of diverse IFNs against the 5 isolates and observed marked differences in IFN sensitivities (Fig 4A). Pairwise analysis of antiviral potencies between isolates collected early (January 2020) and later (March-December 2020) during the pandemic were performed against the 14 IFN-Is (IFN-III data were not included due to low antiviral activity, Fig. 2). The overall IFN-I sensitivity of USA-WA1/2020 and Germany/BavPat1/2020 isolates were not significantly different from each other (Fig 4B). In contrast, relative to Germany/BavPat1/2020, we observed 17 to 122-fold IFN-I resistance of the emerging SARS-CoV-2 variants (Fig 4C), with the B.1.1.7 strain exhibiting the highest IFN-I resistance (this can also be seen in Fig. 3). The level of interferon resistance was especially striking when compared to the early pandemic USA-WA1/2020 strain, where emerging SARS-CoV-2 variants exhibited 25 to 322-fold higher IFN-I resistance (Fig 4D).

142 The experiments to this point allowed for the simultaneous analysis of 17 IFNs against multiple
143 SARS-CoV-2 isolates, but did not provide information on how different IFN-I doses affect virus
144 replication. It also remained unclear if the emerging variants were resistant to IFN-IIIs. We
145 therefore titrated a potent (IFNβ; 0.002 to 200 pM) and a weak (IFNλ1; 0.02 to 2000 pM)
146 interferon against the lineage A, B, B.1, B.1.1.7 and B.1.351 viruses (Fig 5 and S5 Fig). Of note,
147 as the pandemic progressed in the past year, new variants of concern (VOCs) became dominant
148 in several countries; the WHO implemented a simplified Greek letter nomenclature for these
149 VOCs. We therefore included 3 additional VOCs, which were also obtained from the BEI
150 repository: (1) a second B.1.1.7 (alpha) isolate, England/204820464/2020; (2) an isolate from
151 lineage P.1 (gamma), which branched off from lineage B.1.1.28; and (3) an isolate from lineage
152 B.1.617.2 (delta) (S1 Table). Lineage P.1 was first described in an outbreak of SARS-CoV-2 in
153 Manaus, Brazil, which occurred in a population with high levels of prior infection. P.1
154 independently acquired the E484K mutation [25, 26] (Fig 1A, S1 Table). The delta strain was
155 first reported in India in early 2021 [27, 28], and as of July 2021, has become the dominant
156 variant worldwide, including the USA [29]. The delta strain was particularly concerning as it was
157 frequently observed in breakthrough infections among fully-vaccinated individuals [30, 31].
158
159 The lineage A and B isolates were similarly inhibited by IFNβ and IFNλ1 (S5A Fig). Comparing
160 B to B.1, the 50% inhibitory concentration (IC_{50}) of the B.1 isolate was 2.6 and 5.5-fold higher
161 IC_{50} for IFNλ1 and IFNβ, respectively (S5B Fig). Comparing B to B.1.1.7, the B.1.1.7 variants
162 IC_{50}s were 4.3 to 8.3-fold higher for IFNβ and 3.0 to 3.5 higher for IFNλ1 (Fig 5A).
163 Interestingly, maximum inhibition was not achieved with either IFNβ or IFNλ1 against the
164 B.1.1.7 variant, plateauing at 15 to 20-fold higher levels than the ancestral lineage B isolate (Fig.

5A), which was in sharp contrast to the lineage B.1 isolate (S5B Fig). In a separate experiment, the B.1.351 variant was also more resistant to IFNβ (43-fold) and IFNλ1 (26-fold) compared to the lineage B isolate (Fig 5B). Here, however, maximum inhibition was achieved with IFNβ. The P.1 variant also exhibited higher resistance to IFNβ (1.9-fold) and IFNλ1 (4.4-fold), and the plateau concentration for antiviral activity was >10-fold higher for IFNβ than for the lineage B isolate (Fig. 5C). Consistent with the findings with the other VOCs, the B.1.617.2 (delta) variant was also more resistant to IFNβ (6.7-fold) (Fig. 5D). Although similar IC50s were obtained with IFNλ1, the B.1.617.2 isolate had higher residual replication at the highest doses than the ancestral lineage B isolate (Fig. 5D).

Two months after our initial preprint [32], Thorne *et* al posted data that in Calu-3 cells, a B.1.1.7 isolate, was more resistant to IFNβ than a 'first wave' lineage B isolate [33]. We found that lineage A and B isolates replicated poorly in Calu-3 cells, making these cells unsuitable for IFN resistance comparisons between ancestral versus emerging variants (S6A Fig). This was in sharp contrast to A549-ACE2 cells, where we observed high levels of virus production (>10^5 copies) of all strains studied (S1B Fig). Notably, comparable titers were obtained between the B.1 and B.1.1.7 isolates in Calu-3 cells (S6A Fig). In these cells, the B.1.1.7 isolate was 50-fold more resistant to IFNλ1 than the B.1 isolate (S6B Fig). We also demonstrate that the B.1.1.7 and B.1.617.2 isolates were more resistant to IFNβ than the B.1 isolate (S6C Fig). Altogether, our data demonstrate that the B.1, B.1.1.7, B.1.351, P.1 and B.1.617.2 isolates have evolved to resist the IFN-I and IFN-III response.

Discussion

Numerous studies have shown that interferons are important for host defense against SARS-CoV-2. This sarbecovirus is believed to have recently crossed the species barrier to humans, either directly from bats or via an intermediate mammalian host(s) [34]. Here, we demonstrate that SARS-CoV-2 has in fact evolved after host switching to become more resistant to human interferons. Moreover, we establish an order of antiviral potency for the diverse type I and III IFNs. IFNλ initially showed promise as an antiviral that can reduce inflammation [35], but our data suggest that for SARS-CoV-2, higher doses of IFNλ may be needed to achieve a similar antiviral effect *in vivo* as the IFN-Is. Nebulized IFNβ showed potential as a therapeutic against COVID-19 [11], and our data confirm IFNβ is highly potent against SARS-CoV-2. However, IFNβ was also linked to pathogenic outcomes in chronic mucosal HIV-1 [23], murine LCMV [36] and if administered late in mice, SARS-CoV-1 and MERS-CoV [37, 38] infection. We previously reported that IFNβ upregulated 2.4-fold more genes than individual IFNα subtypes, suggesting that IFNβ may induce more pleiotropic effects [23]. Among the IFNα subtypes, IFNα8 showed similar anti-SARS-CoV-2 potency as IFNβ. IFNα8 also exhibited high antiviral activity against HIV-1 [3], raising its potential for treatment against both pandemic viruses. Notably, IFNα8 appeared to be an outlier in this regard, as the antiviral potencies of the IFNα subtypes against SARS-CoV-2 and HIV-1 generally did not strongly correlate (Fig. 3C). IFNα6 potently restricted HIV-1 [3, 4] but was one of the weakest IFNα subtypes against SARS-CoV-2. Conversely, IFNα5 strongly inhibited SARS-CoV-2, but weakly inhibited HIV-1 [3]. This lack of correlation is a key point for future studies. Of note, the high potency of IFNα5 and low potency of IFNα6 against an isolate of SARS-CoV-2 (not a variant of concern) were corroborated by another group [39]. Collectively, these data strengthen the theory that diverse

IFNs may have evolved to restrict distinct virus families [2, 23]. The mechanisms underlying these interesting qualitative differences remain unclear. While IFNAR signaling contributes to antiviral potency [3, 4, 24], diverse IFNs may have distinct abilities to mobilize antiviral effectors in specific cell types. Comparing the interferomes induced by distinct IFNs in lung epithelial cells [39] may be useful in prioritizing further studies on this point.

Most significantly, our data reveal for the first time the concerning trend for SARS-CoV-2 variants emerging later in the pandemic – in the setting of prolific replication of the virus in human populations – to resist the antiviral interferon response. Prior to the present work, the emergence and fixation of variants was linked to enhanced viral infectivity and/or neutralizing antibody evasion due to mutations in the Spike protein [13, 16-18, 40]. However, previous studies with HIV-1 suggested that interferons also can shape the evolution of pandemic viruses [41, 42]. In fact, SARS-CoV-2 infected individuals with either genetic defects in IFN signaling [43] or IFN-reactive autoantibodies [44] had increased risk of developing severe COVID-19. As interferons are critical in controlling early virus infection levels, IFN-resistant SARS-CoV-2 variants may produce higher viral loads that could in turn promote transmission and/or exacerbate pathogenesis. Consistent with this hypothesis, some reports have linked B.1.1.7 with increased viral loads [45, 46] and risk of death [47-49]. Notably, infection with B.1.617.2 may yield even higher viral loads than that B.1.1.7 [50].

In addition to Spike, emerging variants exhibit mutations in nucleocapsid, membrane and nonstructural proteins NSP3, NSP6 and NSP12 (S1 Table). In the case of some early pandemic viruses that pre-dated the emergence of the variants of concern, these viral proteins were

reported to antagonize IFN signaling in cells [51-53]. To specifically map the virus mutations driving IFN-I resistance in emerging variants, it will be important to generate recombinant viruses to isolate specific mutations, singly or in combination, and individually test candidate single viral protein antagonists as well. This would help to confirm, for example, that the D3L mutation in the B.1.1.7 nucleocapsid may facilitate innate immune evasion by increasing the expression of an interferon antagonist, ORF9b [33]. The nucleocapsid D3L mutation was not observed in the B.1.351, P.1 and B.1.617.2 lineages (S1 Table), which exhibited IFN-I and IFN-III resistance in our experiments. B.1.617.2 (delta) has now replaced B.1.1.7 (alpha) as the dominant strain in many countries [27, 29], but delta did not seem to be any more interferon-resistant than alpha in both A549-ACE2 and Calu-3 cells. Notably, the delta isolate we studied here had a deletion in ORF7a, which may counteract interferon signaling [52]; this deletion was not a cell culture artifact as it was also observed in the clinical isolate. Analysis of delta isolates with or without the ORF7a deletion would be needed to determine whether innate immune evasion may be a factor for why the delta VOC has overtaken other lineages. Future studies should facilitate understanding the molecular mechanisms of interferon resistance, its consequences for COVID-19 pathogenesis, and the development of novel therapies that augment innate immune defenses against SARS-CoV-2.

Overall, the current study suggested a role for the innate immune response in driving the evolution of SARS-CoV-2 that could have practical implications for interferon-based therapies. Our findings reinforce the importance of continued full-genome surveillance of SARS-CoV-2, and assessments of emerging variants not only for resistance to vaccine-elicited neutralizing antibodies, but also for evasion of the host interferon response.

256

Materials and Methods

Cell lines. A549 cells were obtained from the American Type Culture Collection (ATCC) and cultured in complete media containing F-12 Ham's media (Corning), 10% fetal bovine serum (Atlanta Biologicals), 1% penicillin/streptomycin/glutamine (Corning). Calu-3 cells were also obtained from ATCC and cultured in DMEM supplemented with 10% fetal bovine serum and 1% penicillin/streptomycin/glutamine (Corning). Both cell lines were maintained at 37°C 5% CO_2. A549 cells were transduced with codon-optimized human ACE2 (Genscript) cloned into pBABE-puro [54] (Addgene). To generate the A549-ACE2 stable cell line, 10^7 HEK293T (ATCC) cells in T-175 flasks were transiently co-transfected with 60 µg mixture of pBABE-puro-ACE2, pUMVC, and pCMV-VSV-G at a 10:9:1 ratio using a calcium phosphate method [55]. Forty-eight hours post transfection, the supernatant was collected, centrifuged at 1000×*g* for 5 min and passed through a 0.45 µm syringe filter to remove cell debris. The filtered virus was mixed with fresh media (30% vol/vol) that included polybrene (Sigma) at a 6 µg/ml final concentration. The virus mixture was added into 6-well plates with 5×10^5 A549 cells/well and media was changed once more after 12 h. Transduced cells were selected in 0.5 µg/ml puromycin for 72 h, and ACE2 expression was confirmed by flow cytometry, western blot and susceptibility to HIV-1ΔEnv/SARS-CoV-2 Spike pseudovirions.

Virus isolates. All experiments with live SARS-CoV-2 were performed in a Biosafety Level-3 (BSL3) facility with powered air-purifying respirators at the University of Colorado Anschutz Medical Campus. The SARS-CoV-2 stocks were obtained from BEI Resources (www.beiresources.org). S1 Table provides detailed information on the source of the material, the catalogue and lot numbers and virus sequence information of both the clinical and cultured

stocks. The viruses were propagated in human A549-ACE2 cells unless indicated and harvested by 72 h to minimize mutations that can occur during passage in cell culture, which were documented particularly in nonhuman primate (Vero) or non-alveolar type II (293T) cell lines [56]. The virus stocks had comparable titers $>10^6$ $TCID_{50}$/ml (S1A Fig) except for the two B.1.1.7 strains (CA_CDC_5574/2020 and England/204820464/2020). The contents of the entire vial (~0.5 ml) were inoculated into 3 T-75 flasks containing 3×10^6 A549-ACE2 cells, except for B.1.1.7 which was inoculated into 1 T-75 flask. The supernatants were collected and spun at 2700×*g* for 5 min to remove cell debris, and frozen at -80°C. The A549-amplified stocks were titered according to the proposed assay format (S1B Fig, Fig 2A). Briefly, 2.5×10^4 A549-ACE2 cells were plated per well in a 48-well plate overnight. The next day, the cells were infected with 300, 30, 3, 0.3, 0.03 and 0.003 µl (serial 10-fold dilution) of amplified virus stock in 300 µl final volume of media for 2 h. The virus was washed twice with PBS, and 500 µl of complete media with the corresponding IFN concentrations were added. After 24 h, supernatants were collected, and cell debris was removed by centrifugation at 3200×*g* for 5 min.

Cell viability. To evaluate if the IFN doses affected cell viability, we utilized an MTT assay. 1.5×10^4 A549-ACE2 cells were plated per well in a 96-well plate and treated with 2000 pM IFNλ1, 2 pM IFNλ1, 200 pM IFNβ, 2 pM IFNβ or untreated. Eight replicates were used per treatment group. As a positive control for cell death, the same number of cells were treated with 30% DMSO. 36 hours after treatment, cell proliferation was assessed using the Vybrant MTT Cell Proliferation Assay Kit (Invitrogen). Media was completely removed from cells and replaced with 100 µl of fresh growth media. 10 µl of 12 mM MTT stock solution was added per well and cells were incubated at 37°C for 4 h. 100 µl SDS-HCl solution was added to each well

and mixed thoroughly. After an additional 3 h incubation at 37°C, the absorbance was measured at 570 nm and blank corrected to a media only control.

SARS-CoV-2 quantitative PCR. For rapid and robust assessments of viral replication, we utilized a real-time quantitative PCR (qPCR) approach. This assay would require less handling of infectious, potentially high-titer SARS-CoV-2 in the BSL3 compared to a VeroE6 plaque assay, as the supernatants can be directly placed in lysis buffer containing guanidinium thiocyanate that would inactivate the virus by at least 4-5 $\log_{10}$ [57]. Importantly, residual IFNs in the culture supernatant could further inhibit virus infection in the VeroE6 plaque assay, compromising the infectious titer read-outs. To measure SARS-CoV-2 levels, total RNA was extracted from 100 µl of culture supernatant using the E.Z.N.A Total RNA Kit I (Omega Bio-Tek) and eluted in 50 µl of RNAse-free water. 5 µl of this extract was used for qPCR. Official CDC SARS-CoV-2 N1 gene primers and TaqMan probe set were used [58] with the Luna Universal Probe One-Step RT-qPCR Kit (New England Biolabs):

Forward primer: `GACCCCAAAATCAGCGAAAT`

Reverse primer: `TCTGGTTACTGCCAGTTGAATCTG`

TaqMan probe: `FAM-ACCCCGCATTACGTTTGGTGGACC-TAMRA`

The sequence of the primers and probes were conserved against the 7 SARS-CoV-2 lineages that were investigated. The real-time qPCR reaction was run on a Bio-Rad CFX96 real-time thermocycler under the following conditions: 55°C 10 mins for reverse transcription, then 95°C 1 min followed by 40 cycles of 95°C 10s and 60°C 30s. The absolute quantification of the N1 copy number was interpolated using a standard curve with 10^7-10^1 serial 10-fold dilution of a control plasmid (nCoV-CDC-Control Plasmid, Eurofins).

VeroE6 Plaque Assay. Virus stocks with a pre-determined virus copy number were evaluated in a conventional VeroE6 plaque assay to determine if the virus titers obtained using both methods correlate. 4×10^5 VeroE6 cells (ATCC) were plated in 6-well plates and allowed to adhere overnight at 37°C. Cells were washed once with PBS and infected with 1 ml of viral stocks serially diluted in 2× MEM complete media (10% FBS, 20 mM HEPES, 2× Pen-Step, 2× NEAA and 2× Sodium Pyruvate) for 1 hr at 37°C. After infection, 1 ml of sterile 2.5% cellulose overlay solution (Sigma, Cat. No. 435244-250G) was added to each well and mixed thoroughly. Cells were incubated at 37°C for an additional 48 hr before the media/overlay was removed and the cells fixed in 4% paraformaldehyde (PFA) for 10 min at room temperature. The PFA was removed and the cells were stained with 1% crystal violet in ethanol for 1 minute and washed three times with distilled water. Plaques were manually counted from each well.

Immunofluorescence Assay. Primary human airway epithelial cells fully differentiated in air-liquid interface cultures [59] were infected with different SARS-CoV-2 variants with or without IFNβ. The apical surface was washed with culture medium daily for quantitative PCR. At 96 h post-infection, the cultures were fixed with 4% PFA and wholemount labeled with anti-Spike antibody (Clone ID007, Cat. No. 40150-R007, Sino Biological) followed by Alexa-Dye conjugated secondary antibody. An LSM 900 confocal microscope (Zeiss) was used to generate composite images of the entire culture surface. Spike+ cells were enumerated using the Cell Counter plugin in the ImageJ Software (NIH).

Antiviral inhibition assay. We used a non-saturating dose of the amplified virus stock for the IFN inhibition assays. These titers were expected to yield ~10^5 copies per 5 µl input RNA extract

(S1B Fig). Recombinant IFNs were obtained from PBL Assay Science. These recombinant IFNs were assayed to be >95% pure by SDS-PAGE according to the manufacturer. In addition to the IFN-Is (12 IFNα subtypes, IFNβ and IFNω), we also evaluated 3 IFNλ subtypes (IFNλ1, IFNλ2, IFNλ3). To normalize the IFNs, we used molar concentrations [23] instead of international units (IU), as IU values were derived from inhibition of encelphalomyocarditis virus, which may not be relevant to SARS-CoV-2. Importantly, molar concentrations were used to normalize the relative signaling potencies of the IFNα subtypes and IFNβ [23, 24]. To find a suitable dose to screen 17 IFNs in parallel, we performed a dose-titration experiment of the USA-WA1/2020 strain with IFNβ and IFNλ1. A dose of 2 pM allowed for maximum discrimination of the antiviral potency IFNβ versus IFNλ1 (S1C Fig). Thus, this dose should be within the dynamic range of inhibition of the diverse IFNs investigated. Serial 10-fold dilutions of IFNβ and IFNλ1 were also used in follow-up experiments. Thus, in 48-well plates, we pre-incubated 2.5×10^4 A549-ACE2 cells with the IFNs for 18 h, then infected with the A549-amplified virus stock for 2 h. After two washes with PBS, 500 µl complete media containing the corresponding IFNs were added. The cultures were incubated for another 24 h, after which, supernatants were harvested for RNA extraction and qPCR analysis. A similar procedure was employed for Calu-3 cells, except that IFNλ1 was replenished at 2 dpi and supernatants harvested at day 3.

Statistical analyses. Data were analyzed using GraphPad Prism 8. Differences between the IFNs were tested using a nonparametric two-way analysis of variance (ANOVA) followed by a multiple comparison using the Friedman test. Pearson correlation coefficients (R^2) values were computed for linear regression analyses. Paired analysis of two isolates against multiple IFNs were performed using a nonparametric, two-tailed Wilcoxon matched-pairs rank test. Differences

373 with $p<0.05$ were considered significant. Nonlinear regression curves were used to fit using

374 either a one-site total or two-phase exponential decay equation on log-transformed data.

375

376

Acknowledgments

We thank Cara Wilson, Ulf Dittmer and Kathrin Gibbert for scientific advice; Mercedes Rincon and Elan Eisenmesser for assistance with construction and characterization of the A549-ACE2 cells; Zach Wilson, Jill Garvey, Stephanie Torres-Nemeti, Brett Haltiwanger and Marcia Finucane for Biosafety Level-3 infrastructure support; and Roman Wölfel, Rosina Ehmann, Adolfo García-Sastre, Alex Sigal, Tulio de Oliveira, Bassam Hallis, Matsuyo Takayama-Ito, Richard Webby, Anami Patel, Cathleen Seager, BEI Resources (NIAID) and the CDC for the SARS-CoV-2 isolates.

Funding

This work was supported by the Division of Infectious Diseases, Department of Medicine, University of Colorado (MLS and EMP), the National Institutes of Health R01 AI134220 (MLS), and the Intramural Research Program at the National Institute of Allergy and Infectious Diseases, National Institutes of Health (KJH). The funders had no role in study design, data collection and analysis, decision to publish, or preparation of the manuscript.

Figures

Figure 1. Selection of SARS-CoV-2 strains for IFN sensitivity studies. (A) Global distribution of SARS-CoV-2 clades. GISAID.org plotted the proportion of deposited sequences in designated clades against collection dates. The six isolates chosen are noted by colored dots. (B) SARS-CoV-2 strains selected for this study included representatives of lineages A, B, B.1, B.1.351 and B.1.1.7 (S1 Table). Lineage P.1 (which branched off from lineage B.1.1.28) and B.1.617.2 were added after the initial manuscript submission; and was evaluated for IFNβ and IFNλ1 sensitivity. Lineage B isolates encode the D614G mutation associated with increased transmissibility. Note that the B.1.1.7 strain was later updated to belong to the GISAID clade, 'GRY'. *Amino acid mutations were relative to the reference hCOV-19/Wuhan/WIV04/2019 sequence.

Figure 2. Sensitivity of SARS-CoV-2 strains to IFN-I and IFN-III interferons. (A) Antiviral assay using recombinant IFNs (2 pM) in A549-ACE2 cells. The red line corresponds to the qPCR detection limit (90 copies/reaction, or 1.8 x 10^4 copies/ml). (B) Viral copy numbers in D614G+ isolates, showing a similar rank-order of IFNs from least to most potent. (C) The average fold-inhibition relative to mock for lineage B, B.1, B.1.351 and B.1.1.7 isolates are shown. The most potent IFNs are shown top to bottom. For all panels, bars and error bars correspond to means and standard deviations.

Figure 3. Correlation between SARS-CoV-2 inhibition and biological properties of IFNα subtypes. Log-transformed IFN-inhibition values relative to mock for the 5 different SARS-CoV-2 strains were compared to previously published values on (A) 50% effective

concentrations in the iLite assay, a reporter cell line encoding the IFN sensitive response element of *ISG15* linked to firefly luciferase [23]; (B) IFNAR2 subunit binding affinity, as measured by surface plasmon resonance by the Schreiber group [24]; and (C) HIV-1 inhibition values, based on % inhibition of HIV-1 p24+ gut lymphocytes relative to mock as measured by flow cytometry [3]. Each dot corresponds to an IFNα subtype. Linear regression was performed using GraphPad Prism 8. Significant correlations ($p<0.05$) were highlighted with a red best-fit line; those that were trending ($p<0.1$) had a gray, dotted best-fit line.

Figure 4. Increased IFN-I resistance of emerging SARS-CoV-2 variants. (A) Heatmap of fold-inhibition of representative strains from the lineages noted. Colors were graded on a log-scale from highest inhibition (yellow) to no inhibition (black). Comparison of IFN-I sensitivities between (B) lineage A and B isolates; (C) lineage B versus B.1, B.1.351 and B.1.1.7 and (D) lineage A versus B.1, B.1.351 and B.1.1.7. The mean fold-inhibition values relative to mock were compared in a pairwise fashion for the 14 IFN-Is. In (C) and (D), the average fold-inhibition values were noted. Differences were evaluated using a nonparametric, two-tailed Wilcoxon matched-pairs signed rank test. NS, not significant; ****, $p<0.0001$.

Figure 5. Dose-titration of ancestral lineage B versus four variants of concern against IFNβ and IFNλ1. Data from four separate experiments (panels A-D) are shown. (A) Dose-titration of IFNβ and IFNλ1 against lineage B (Germany/BavPat1/2020) versus B.1.1.7 (alpha) isolates. In addition to USA/CA_CDC_5574/2020, we also evaluated a second B.1.1.7 isolate from the United Kingdom (UK), England/204820464/2020. *The value at 200 pM IFNλ1 for the lineage B isolate was 0.54, precluding efforts for finding a best-fit curve for IC50 determination; this

datapoint was therefore not included in the curve fitting. (B) IC50 comparison between a lineage B (Germany/BavPat1/2020) and a B.1.351 (beta) isolate (South Africa/KRISP-EC-K005321/2020). (C) IC50 comparison between a lineage B isolate (Germany/BavPat1/2020) and a P.1 (gamma) isolate (Japan/TY7-503/2021). (D) IC50 comparison between a lineage B isolate (Germany/BavPat1/2020) and a B.1.617.2 (delta) isolate (USA/PHC658/2021). For all panels, A549-ACE2 cells were pre-treated with serial 10-fold dilutions of IFNs for 18 h in triplicate and then infected with SARS-CoV-2. Supernatants were collected after 24 h, SARS-CoV-2 N1 copy numbers were determined by qPCR in triplicate, and then the mean copy numbers were normalized against mock as 100%. Error bars correspond to standard deviations. Non-linear best-fit regression curves of mean normalized infection levels were used to interpolate 50% inhibitory concentrations (green dotted lines).

References

1. Pestka S, Krause CD, Walter MR. Interferons, interferon-like cytokines, and their receptors. Immunol Rev. 2004;202:8-32. Epub 2004/11/18.
2. Gibbert K, Schlaak JF, Yang D, Dittmer U. IFN-alpha subtypes: distinct biological activities in anti-viral therapy. British journal of pharmacology. 2013;168(5):1048-58.
3. Harper MS, Guo K, Gibbert K, Lee EJ, Dillon SM, Barrett BS, et al. Interferon-alpha Subtypes in an Ex Vivo Model of Acute HIV-1 Infection: Expression, Potency and Effector Mechanisms. PLoS pathogens. 2015;11(11):e1005254.
4. Schlaepfer E, Fahrny A, Gruenbach M, Kuster SP, Simon V, Schreiber G, et al. Dose-Dependent Differences in HIV Inhibition by Different Interferon Alpha Subtypes While Having Overall Similar Biologic Effects. mSphere. 2019;4(1). Epub 2019/02/15.
5. Lavender KJ, Gibbert K, Peterson KE, Van Dis E, Francois S, Woods T, et al. Interferon Alpha Subtype-Specific Suppression of HIV-1 Infection In Vivo. Journal of virology. 2016;90(13):6001-13.
6. Matos ADR, Wunderlich K, Schloer S, Schughart K, Geffers R, Seders M, et al. Antiviral potential of human IFN-alpha subtypes against influenza A H3N2 infection in human lung explants reveals subtype-specific activities. Emerg Microbes Infect. 2019;8(1):1763-76.
7. Vanderheiden A, Ralfs P, Chirkova T, Upadhyay AA, Zimmerman MG, Bedoya S, et al. Type I and Type III Interferons Restrict SARS-CoV-2 Infection of Human Airway Epithelial Cultures. Journal of virology. 2020;94(19). Epub 2020/07/24.
8. Felgenhauer U, Schoen A, Gad HH, Hartmann R, Schaubmar AR, Failing K, et al. Inhibition of SARS-CoV-2 by type I and type III interferons. The Journal of biological chemistry. 2020;295(41):13958-64. Epub 2020/06/27.
9. Nchioua R, Kmiec D, Muller JA, Conzelmann C, Gross R, Swanson CM, et al. SARS-CoV-2 Is Restricted by Zinc Finger Antiviral Protein despite Preadaptation to the Low-CpG Environment in Humans. mBio. 2020;11(5). Epub 2020/10/18.
10. Wang N, Zhan Y, Zhu L, Hou Z, Liu F, Song P, et al. Retrospective Multicenter Cohort Study Shows Early Interferon Therapy Is Associated with Favorable Clinical Responses in COVID-19 Patients. Cell host & microbe. 2020;28(3):455-64 e2. Epub 2020/07/25.
11. Monk PD, Marsden RJ, Tear VJ, Brookes J, Batten TN, Mankowski M, et al. Safety and efficacy of inhaled nebulised interferon beta-1a (SNG001) for treatment of SARS-CoV-2 infection: a randomised, double-blind, placebo-controlled, phase 2 trial. Lancet Respir Med. 2020. Epub 2020/11/16.
12. Shalhoub S. Interferon beta-1b for COVID-19. Lancet. 2020;395(10238):1670-1. Epub 2020/05/14.
13. Rambaut A, Holmes EC, O'Toole A, Hill V, McCrone JT, Ruis C, et al. A dynamic nomenclature proposal for SARS-CoV-2 lineages to assist genomic epidemiology. Nat Microbiol. 2020;5(11):1403-7. Epub 2020/07/17.
14. Zhou P, Yang XL, Wang XG, Hu B, Zhang L, Zhang W, et al. A pneumonia outbreak associated with a new coronavirus of probable bat origin. Nature. 2020;579(7798):270-3.

15. Worobey M, Pekar J, Larsen BB, Nelson MI, Hill V, Joy JB, et al. The emergence of SARS-CoV-2 in Europe and North America. Science (New York, NY. 2020;370(6516):564-70. Epub 2020/09/12.

16. Korber B, Fischer WM, Gnanakaran S, Yoon H, Theiler J, Abfalterer W, et al. Tracking Changes in SARS-CoV-2 Spike: Evidence that D614G Increases Infectivity of the COVID-19 Virus. Cell. 2020;182(4):812-27 e19. Epub 2020/07/23.

17. Plante JA, Liu Y, Liu J, Xia H, Johnson BA, Lokugamage KG, et al. Spike mutation D614G alters SARS-CoV-2 fitness. Nature. 2020. Epub 2020/10/28.

18. Hou YJ, Chiba S, Halfmann P, Ehre C, Kuroda M, Dinnon KH, 3rd, et al. SARS-CoV-2 D614G variant exhibits efficient replication ex vivo and transmission in vivo. Science (New York, NY. 2020;370(6523):1464-8. Epub 2020/11/14.

19. Gonzalez-Reiche AS, Hernandez MM, Sullivan MJ, Ciferri B, Alshammary H, Obla A, et al. Introductions and early spread of SARS-CoV-2 in the New York City area. Science (New York, NY. 2020;369(6501):297-301. Epub 2020/05/31.

20. Wibmer CK, Ayres F, Hermanus T, Madzivhandila M, Kgagudi P, Oosthuysen B, et al. SARS-CoV-2 501Y.V2 escapes neutralization by South African COVID-19 donor plasma. Nature medicine. 2021. Epub 2021/03/04.

21. Wang P, Nair MS, Liu L, Iketani S, Luo Y, Guo Y, et al. Antibody Resistance of SARS-CoV-2 Variants B.1.351 and B.1.1.7. Nature. 2021. Epub 2021/03/09.

22. Galloway SE, Paul P, MacCannell DR, Johansson MA, Brooks JT, MacNeil A, et al. Emergence of SARS-CoV-2 B.1.1.7 Lineage - United States, December 29, 2020-January 12, 2021. MMWR Morb Mortal Wkly Rep. 2021;70(3):95-9. Epub 2021/01/22.

23. Guo K, Shen G, Kibbie J, Gonzalez T, Dillon SM, Smith HA, et al. Qualitative Differences Between the IFNalpha subtypes and IFNbeta Influence Chronic Mucosal HIV-1 Pathogenesis. PLoS pathogens. 2020;16(10):e1008986. Epub 2020/10/17.

24. Lavoie TB, Kalie E, Crisafulli-Cabatu S, Abramovich R, DiGioia G, Moolchan K, et al. Binding and activity of all human alpha interferon subtypes. Cytokine. 2011;56(2):282-9.

25. Faria NR, Mellan TA, Whittaker C, Claro IM, Candido DDS, Mishra S, et al. Genomics and epidemiology of the P.1 SARS-CoV-2 lineage in Manaus, Brazil. Science (New York, NY. 2021;372(6544):815-21. Epub 2021/04/16.

26. Naveca FG, Nascimento V, de Souza VC, Corado AL, Nascimento F, Silva G, et al. COVID-19 in Amazonas, Brazil, was driven by the persistence of endemic lineages and P.1 emergence. Nature medicine. 2021. Epub 2021/05/27.

27. Mlcochova P, Kemp S, Dhar MS, Papa G, Meng B, Mishra S, et al. SARS-CoV-2 B.1.617.2 Delta variant emergence and vaccine breakthrough. Research Square Platform LLC.

28. Singh J, Rahman SA, Ehtesham NZ, Hira S, Hasnain SE. SARS-CoV-2 variants of concern are emerging in India. Nature medicine. 2021;27(7):1131-3. Epub 2021/05/29.

29. Monitoring Variant Proportions [Internet]. 2021. Available from: https://covid.cdc.gov/covid-data-tracker/#variant-proportions.

30. Chia PY, Ong SWX, Chiew CJ, Ang LW, Chavatte JM, Mak TM, et al. Virological and serological kinetics of SARS-CoV-2 Delta variant vaccine-breakthrough infections: a multi-center cohort study. medRxiv. 2021.

31. Brown CM, Vostok J, Johnson H, Burns M, Gharpure R, Sami S, et al. Outbreak of SARS-CoV-2 Infections, Including COVID-19 Vaccine Breakthrough Infections, Associated with Large Public Gatherings - Barnstable County, Massachusetts, July 2021. MMWR Morb Mortal Wkly Rep. 2021;70(31):1059-62. Epub 2021/08/06.

32. Guo K, Barrett BS, Mickens KL, Hasenkrug KJ, Santiago ML. Interferon Resistance of Emerging SARS-CoV-2 Variants. bioRxiv. 2021. Epub 2021/03/25.

33. Thorne LG, Bouhaddou M, Reuschl AK, Zuliani-Alvarez L, Polacco B, Pelin A, et al. Evolution of enhanced innate immune evasion by the SARS-CoV-2 B.1.1.7 UK variant. bioRxiv. 2021. Epub 2021/06/16.

34. Holmes EC, Goldstein SA, Rasmussen AL, Robertson DL, Crits-Christoph A, Wertheim JO, et al. The origins of SARS-CoV-2: A critical review. Cell. 2021. Epub 2021/09/05.

35. Davidson S, McCabe TM, Crotta S, Gad HH, Hessel EM, Beinke S, et al. IFNlambda is a potent anti-influenza therapeutic without the inflammatory side effects of IFNalpha treatment. EMBO molecular medicine. 2016;8(9):1099-112.

36. Ng CT, Sullivan BM, Teijaro JR, Lee AM, Welch M, Rice S, et al. Blockade of interferon Beta, but not interferon alpha, signaling controls persistent viral infection. Cell host & microbe. 2015;17(5):653-61.

37. Channappanavar R, Fehr AR, Zheng J, Wohlford-Lenane C, Abrahante JE, Mack M, et al. IFN-I response timing relative to virus replication determines MERS coronavirus infection outcomes. J Clin Invest. 2019;130:3625-39.

38. Channappanavar R, Fehr AR, Vijay R, Mack M, Zhao J, Meyerholz DK, et al. Dysregulated Type I Interferon and Inflammatory Monocyte-Macrophage Responses Cause Lethal Pneumonia in SARS-CoV-Infected Mice. Cell host & microbe. 2016;19(2):181-93.

39. Schuhenn J, Meister TL, Todt D, Bracht T, Schork K, Billaud J-N, et al. Differential interferon-alpha subtype immune signatures suppress SARS-CoV-2 infection. BioRxiv. 2021.

40. Weisblum Y, Schmidt F, Zhang F, DaSilva J, Poston D, Lorenzi JC, et al. Escape from neutralizing antibodies by SARS-CoV-2 spike protein variants. Elife. 2020;9. Epub 2020/10/29.

41. Iyer SS, Bibollet-Ruche F, Sherrill-Mix S, Learn GH, Plenderleith L, Smith AG, et al. Resistance to type 1 interferons is a major determinant of HIV-1 transmission fitness. Proceedings of the National Academy of Sciences of the United States of America. 2017;114(4):E590-E9. Epub 2017/01/11.

42. Parrish NF, Gao F, Li H, Giorgi EE, Barbian HJ, Parrish EH, et al. Phenotypic properties of transmitted founder HIV-1. Proceedings of the National Academy of Sciences of the United States of America. 2013;110(17):6626-33.

43. Zhang Q, Bastard P, Liu Z, Le Pen J, Moncada-Velez M, Chen J, et al. Inborn errors of type I IFN immunity in patients with life-threatening COVID-19. Science (New York, NY. 2020;370(6515). Epub 2020/09/26.

44. Bastard P, Rosen LB, Zhang Q, Michailidis E, Hoffmann HH, Zhang Y, et al. Autoantibodies against type I IFNs in patients with life-threatening COVID-19. Science (New York, NY. 2020;370(6515). Epub 2020/09/26.

45. Kidd M, Richter A, Best A, Cumley N, Mirza J, Percival B, et al. S-variant SARS-CoV-2 lineage B1.1.7 is associated with significantly higher viral loads in samples tested by ThermoFisher TaqPath RT-qPCR. The Journal of infectious diseases. 2021. Epub 2021/02/14.

46. Frampton D, Rampling T, Cross A, Bailey H, Heaney J, Byott M, et al. Genomic characteristics and clinical effect of the emergent SARS-CoV-2 B.1.1.7 lineage in London, UK: a whole-genome sequencing and hospital-based cohort study. Lancet Infectious Diseases. 2021.

47. Grint DJ, Wing K, Williamson E, McDonald HI, Bhaskaran K, Evans D, et al. Case fatality risk of the SARS-CoV-2 variant of concern B.1.1.7 in England, 16 November to 5 February. Euro Surveill. 2021;26(11). Epub 2021/03/20.

48. Davies NG, Jarvis CI, Group CC-W, Edmunds WJ, Jewell NP, Diaz-Ordaz K, et al. Increased mortality in community-tested cases of SARS-CoV-2 lineage B.1.1.7. Nature. 2021. Epub 2021/03/17.

49. Challen R, Brooks-Pollock E, Read JM, Dyson L, Tsaneva-Atanasova K, Danon L. Risk of mortality in patients infected with SARS-CoV-2 variant of concern 202012/1: matched cohort study. BMJ. 2021;372:n579. Epub 2021/03/11.

50. Ong SWX, Chiew CJ, Ang LW, Mak TM, Cui L, Toh M, et al. Clinical and virological features of SARS-CoV-2 variants of concern: a retrospective cohort study comparing B.1.1.7 (Alpha), B.1.315 (Beta), and B.1.617.2 (Delta). Clin Infect Dis. 2021. Epub 2021/08/24.

51. Lei X, Dong X, Ma R, Wang W, Xiao X, Tian Z, et al. Activation and evasion of type I interferon responses by SARS-CoV-2. Nat Commun. 2020;11(1):3810. Epub 2020/08/01.

52. Xia H, Cao Z, Xie X, Zhang X, Chen JY, Wang H, et al. Evasion of Type I Interferon by SARS-CoV-2. Cell reports. 2020;33(1):108234. Epub 2020/09/28.

53. Mu J, Fang Y, Yang Q, Shu T, Wang A, Huang M, et al. SARS-CoV-2 N protein antagonizes type I interferon signaling by suppressing phosphorylation and nuclear translocation of STAT1 and STAT2. Cell Discov. 2020;6:65. Epub 2020/09/22.

54. Morgenstern JP, Land H. Advanced mammalian gene transfer: high titre retroviral vectors with multiple drug selection markers and a complementary helper-free packaging cell line. Nucleic acids research. 1990;18(12):3587-96. Epub 1990/06/25.

55. Dillon SM, Guo K, Castleman MJ, Santiago ML, Wilson CC. Quantifying HIV-1-Mediated Gut CD4+ T Cell Death in the Lamina Propria Aggregate Culture (LPAC) Model Bio-Protocol. 2020;10(2).

608 56. Sasaki M, Uemura K, Sato A, Toba S, Sanaki T, Maenaka K, et al. SARS-CoV-2 variants
609 with mutations at the S1/S2 cleavage site are generated in vitro during propagation in
610 TMPRSS2-deficient cells. PLoS pathogens. 2021;17(1):e1009233. Epub 2021/01/22.

611 57. Pastorino B, Touret F, Gilles M, Luciani L, de Lamballerie X, Charrel RN. Evaluation of
612 Chemical Protocols for Inactivating SARS-CoV-2 Infectious Samples. Viruses. 2020;12(6).
613 Epub 2020/06/12.

614 58. CDC. Research Use Only 2019-Novel Coronavirus (2019-nCoV) Real-time RT-PCR Primers
615 and Probes. https://www.cdc.gov/coronavirus/2019-ncov/lab/rt-pcr-panel-primer-
616 probes.html. 2020.

617 59. Robinot R, Hubert M, de Melo GD, Lazarini F, Bruel T, Smith N, et al. SARS-CoV-2
618 infection induces the dedifferentiation of multiciliated cells and impairs mucociliary
619 clearance. Nat Commun. 2021;12(1):4354. Epub 2021/07/18.

620

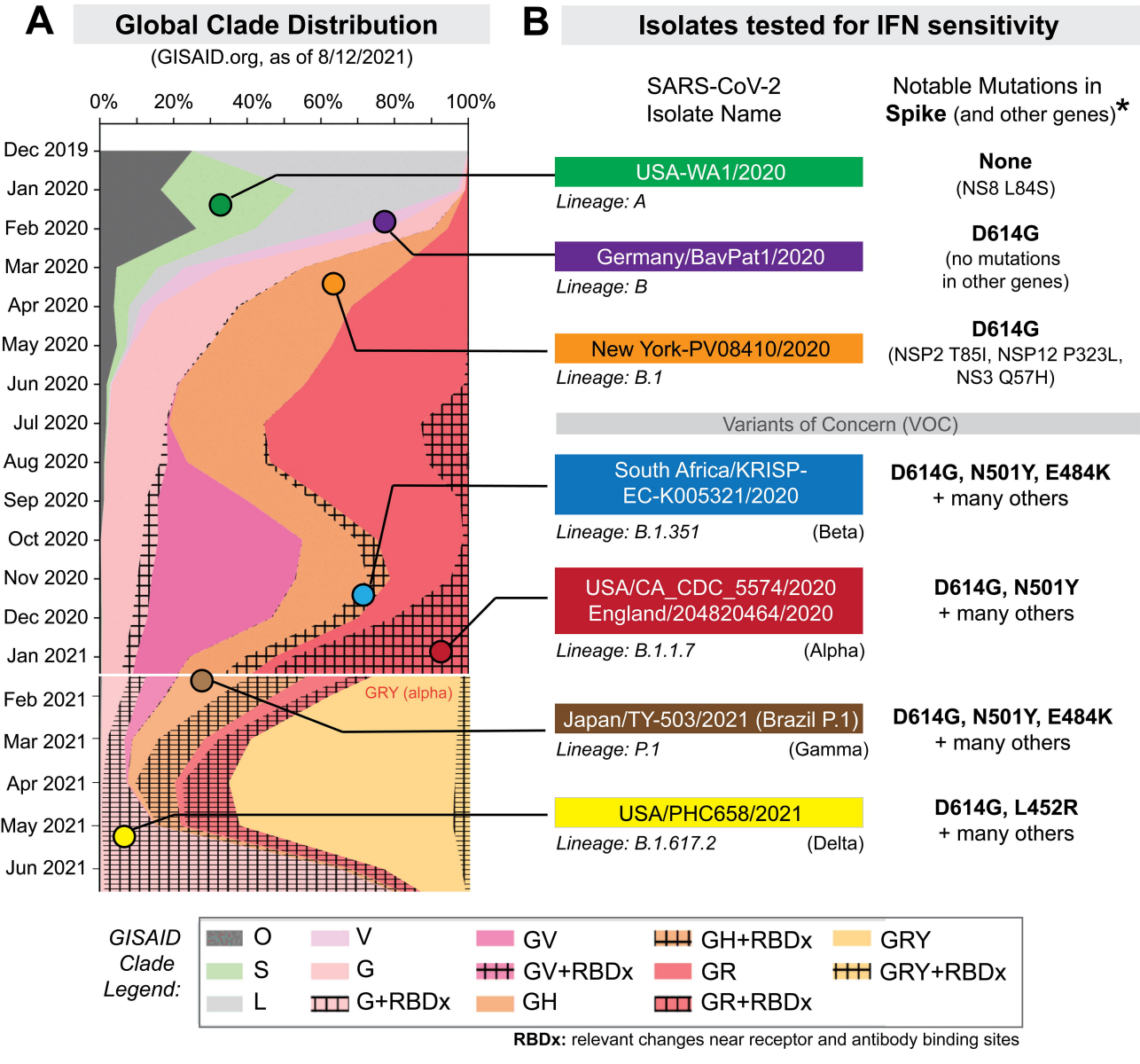
A
Global Clade Distribution
(GISAID.org, as of 8/12/2021)
0%
20%
40%
60%
80%
100%
Dec 2019
Jan 2020
Feb 2020
Mar 2020
Apr 2020
May 2020
Jun 2020
Jul 2020
Aug 2020
Sep 2020
Oct 2020
Nov 2020
Dec 2020
Jan 2021
Feb 2021
Mar 2021
Apr 2021
May 2021
Jun 2021
GRY (alpha)
B
Isolates tested for IFN sensitivity
SARS-CoV-2 Isolate Name
Notable Mutations in Spike (and other genes)*
USA-WA1/2020
Lineage: A
None
(NS8 L84S)
Germany/BavPat1/2020
Lineage: B
D614G
(no mutations in other genes)
New York-PV08410/2020
Lineage: B.1
D614G
(NSP2 T85I, NSP12 P323L, NS3 Q57H)
Variants of Concern (VOC)
South Africa/KRISP-EC-K005321/2020
Lineage: B.1.351 (Beta)
D614G, N501Y, E484K
+ many others
USA/CA_CDC_5574/2020
England/204820464/2020
Lineage: B.1.1.7 (Alpha)
D614G, N501Y
+ many others
Japan/TY-503/2021 (Brazil P.1)
Lineage: P.1 (Gamma)
D614G, N501Y, E484K
+ many others
USA/PHC658/2021
Lineage: B.1.617.2 (Delta)
D614G, L452R
+ many others
GISAID Clade Legend:
O
S
L
V
G
G+RBDx
GV
GV+RBDx
GH
GH+RBDx
GR
GR+RBDx
GRY
GRY+RBDx
RBDx: relevant changes near receptor and antibody binding sites

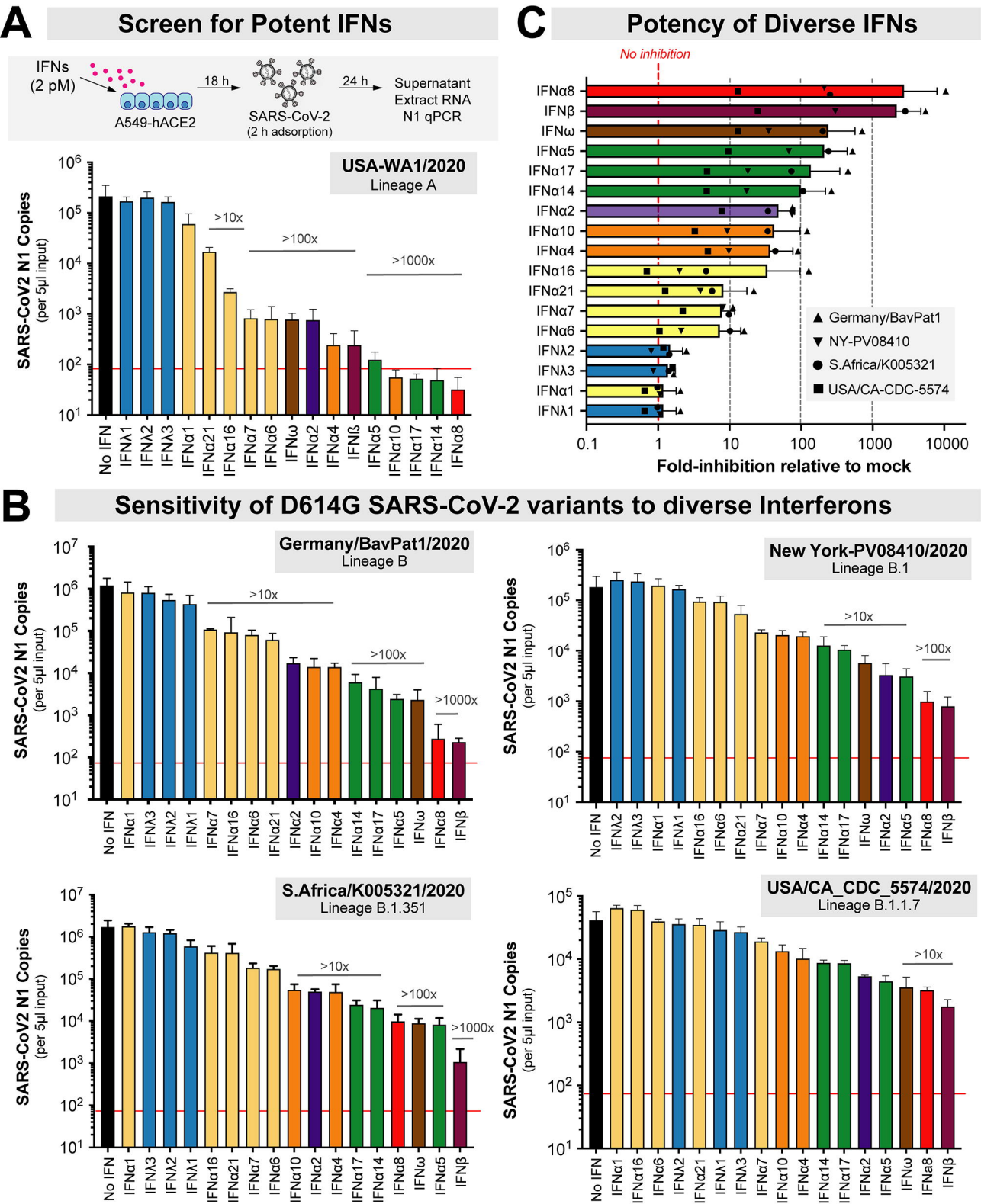
A
Screen for Potent IFNs
IFNs
(2 pM)
A549-hACE2
18 h
SARS-CoV-2
(2 h adsorption)
24 h
Supernatant
Extract RNA
N1 qPCR
USA-WA1/2020
Lineage A
SARS-CoV2 N1 Copies
(per 5µl input)
>10x
>100x
>1000x
No IFN
IFNλ1
IFNλ2
IFNλ3
IFNα1
IFNα21
IFNα16
IFNα7
IFNα6
IFNω
IFNα2
IFNα4
IFNß
IFNα5
IFNα10
IFNα17
IFNα14
IFNα8
C
Potency of Diverse IFNs
No inhibition
IFNα8
IFNβ
IFNω
IFNα5
IFNα17
IFNα14
IFNα2
IFNα10
IFNα4
IFNα16
IFNα21
IFNα7
IFNα6
IFNλ2
IFNλ3
IFNα1
IFNλ1
Germany/BavPat1
NY-PV08410
S.Africa/K005321
USA/CA-CDC-5574
0.1
1
10
100
1000
10000
Fold-inhibition relative to mock
B
Sensitivity of D614G SARS-CoV-2 variants to diverse Interferons
Germany/BavPat1/2020
Lineage B
New York-PV08410/2020
Lineage B.1
S.Africa/K005321/2020
Lineage B.1.351
USA/CA_CDC_5574/2020
Lineage B.1.1.7

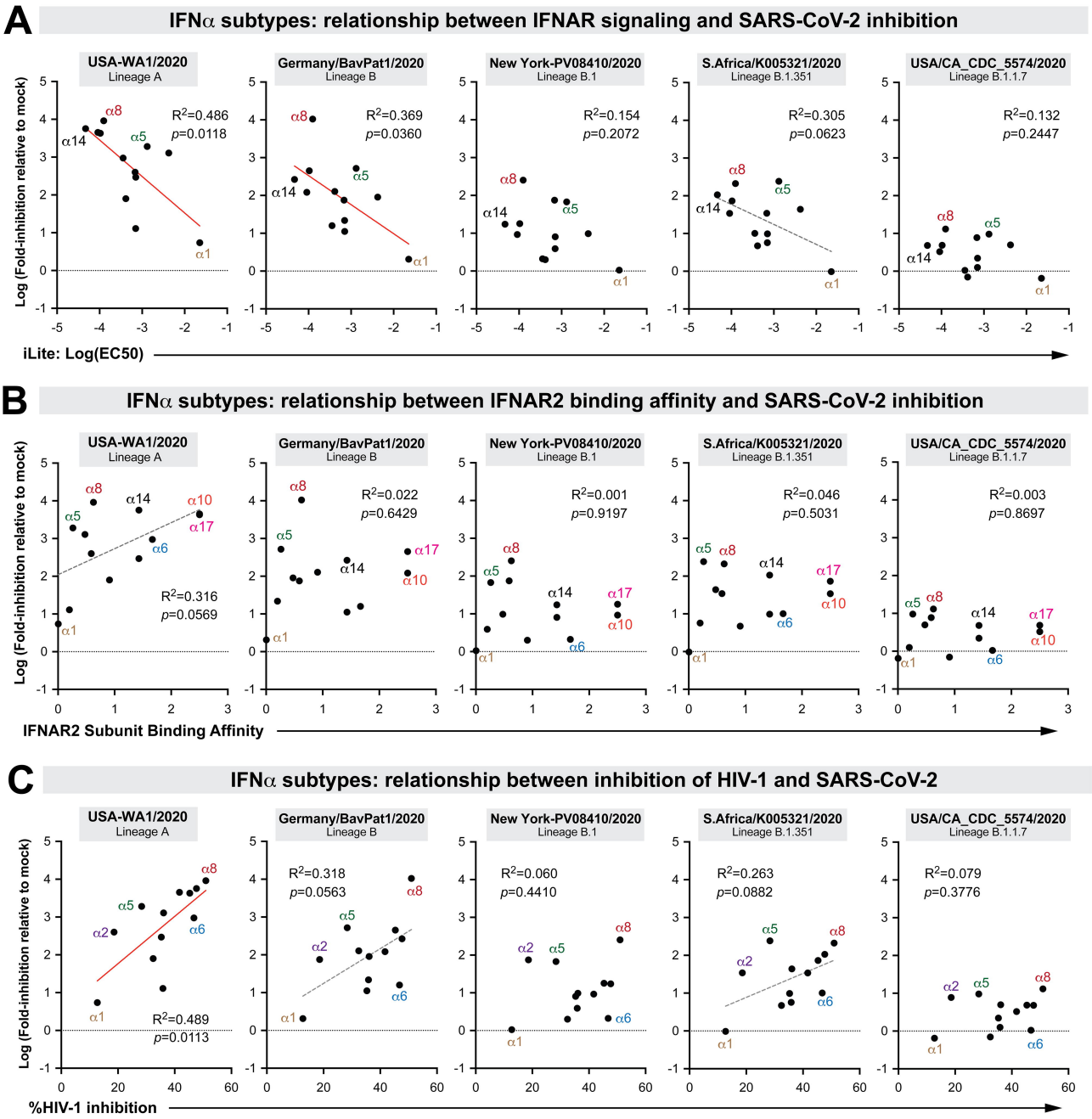
A
IFNα subtypes: relationship between IFNAR signaling and SARS-CoV-2 inhibition
USA-WA1/2020
Lineage A
R²=0.486
p=0.0118
Germany/BavPat1/2020
Lineage B
R²=0.369
p=0.0360
New York-PV08410/2020
Lineage B.1
R²=0.154
p=0.2072
S.Africa/K005321/2020
Lineage B.1.351
R²=0.305
p=0.0623
USA/CA_CDC_5574/2020
Lineage B.1.1.7
R²=0.132
p=0.2447
Log (Fold-inhibition relative to mock)
iLite: Log(EC50)
B
IFNα subtypes: relationship between IFNAR2 binding affinity and SARS-CoV-2 inhibition
R²=0.316
p=0.0569
R²=0.022
p=0.6429
R²=0.001
p=0.9197
R²=0.046
p=0.5031
R²=0.003
p=0.8697
IFNAR2 Subunit Binding Affinity
C
IFNα subtypes: relationship between inhibition of HIV-1 and SARS-CoV-2
R²=0.489
p=0.0113
R²=0.318
p=0.0563
R²=0.060
p=0.4410
R²=0.263
p=0.0882
R²=0.079
p=0.3776
%HIV-1 inhibition

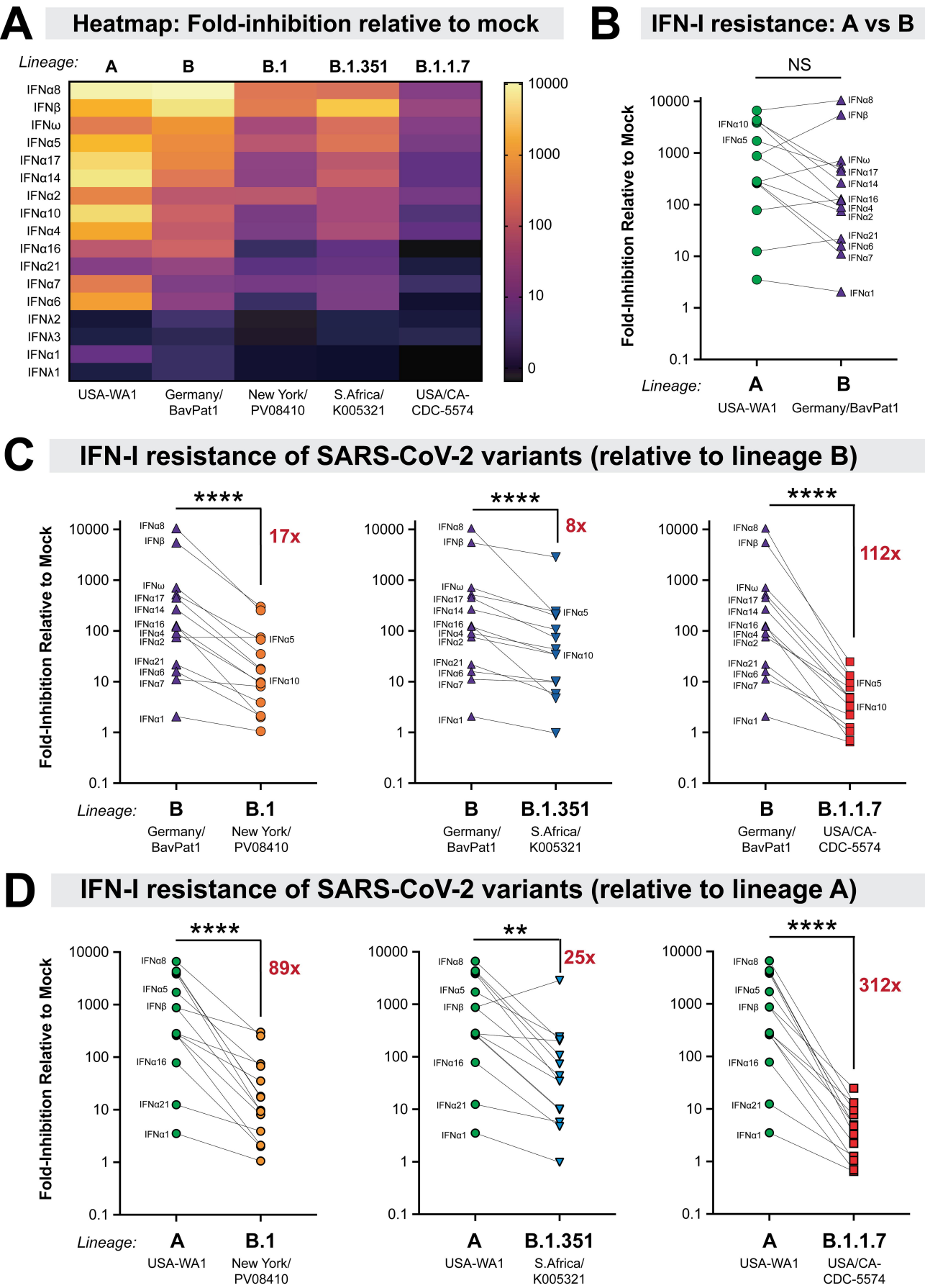
A
Heatmap: Fold-inhibition relative to mock
Lineage:
A
B
B.1
B.1.351
B.1.1.7
IFNα8
IFNβ
IFNω
IFNα5
IFNα17
IFNα14
IFNα2
IFNα10
IFNα4
IFNα16
IFNα21
IFNα7
IFNα6
IFNλ2
IFNλ3
IFNα1
IFNλ1
10000
1000
100
10
0
USA-WA1
Germany/ BavPat1
New York/ PV08410
S.Africa/ K005321
USA/CA- CDC-5574
B
IFN-I resistance: A vs B
NS
Fold-Inhibition Relative to Mock
Lineage:
A
B
USA-WA1
Germany/BavPat1
C
IFN-I resistance of SARS-CoV-2 variants (relative to lineage B)
****
17x
8x
112x
Fold-Inhibition Relative to Mock
Lineage:
B
B.1
Germany/ BavPat1
New York/ PV08410
B.1.351
S.Africa/ K005321
B.1.1.7
USA/CA- CDC-5574
D
IFN-I resistance of SARS-CoV-2 variants (relative to lineage A)
****
**
89x
25x
312x
Fold-Inhibition Relative to Mock
Lineage:
A
B.1
USA-WA1
New York/ PV08410
B.1.351
S.Africa/ K005321
B.1.1.7
USA/CA- CDC-5574

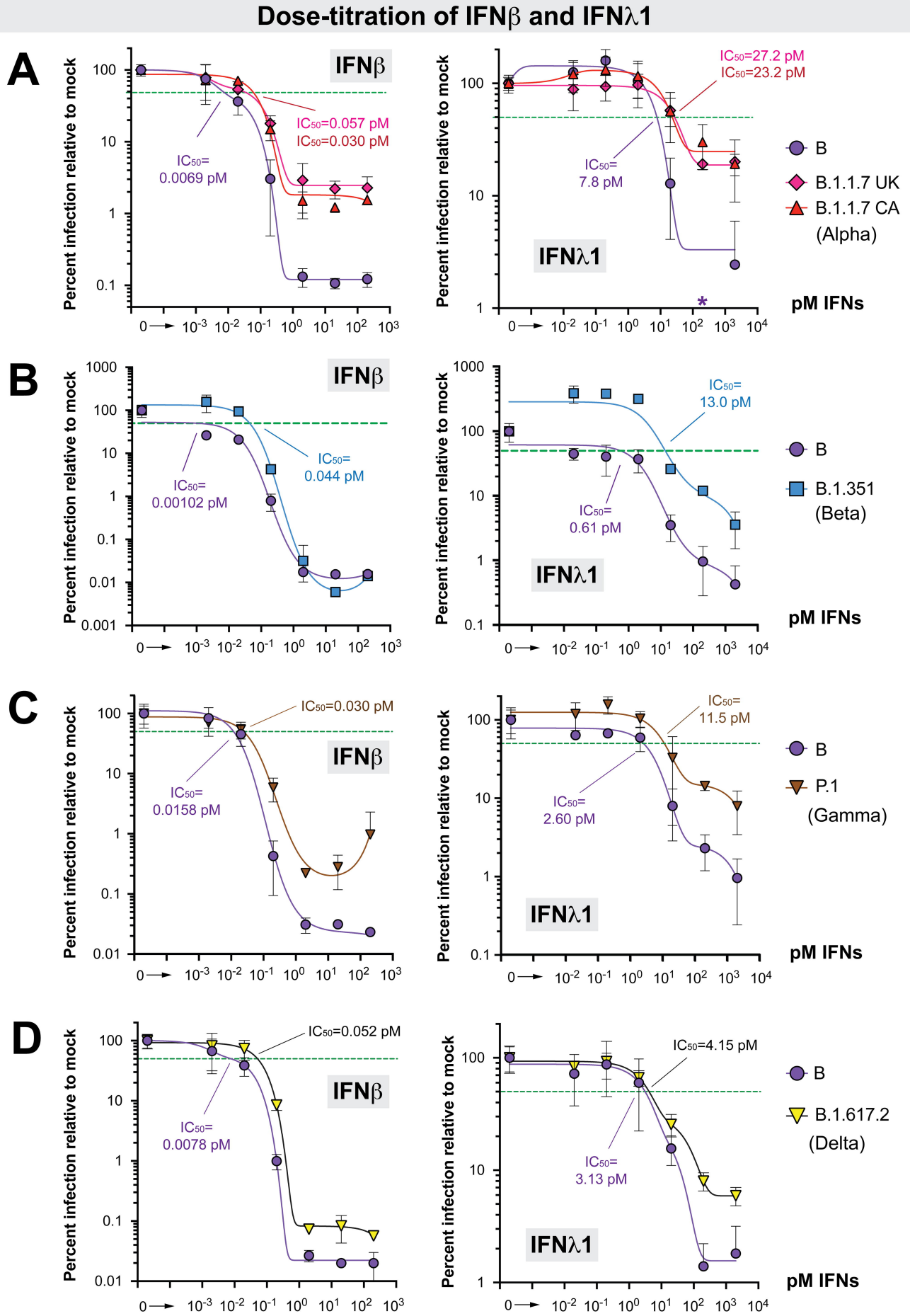
Dose-titration of IFNβ and IFNλ1
A
IFNβ
IC50=0.057 pM
IC50=0.030 pM
IC50= 0.0069 pM
IC50=27.2 pM
IC50=23.2 pM
IC50= 7.8 pM
IFNλ1
B
B.1.1.7 UK
B.1.1.7 CA (Alpha)
pM IFNs
Percent infection relative to mock
B
IFNβ
IC50= 0.044 pM
IC50= 0.00102 pM
IC50= 13.0 pM
IC50= 0.61 pM
IFNλ1
B
B.1.351 (Beta)
pM IFNs
C
IFNβ
IC50=0.030 pM
IC50= 0.0158 pM
IC50= 11.5 pM
IC50= 2.60 pM
IFNλ1
B
P.1 (Gamma)
pM IFNs
D
IFNβ
IC50=0.052 pM
IC50= 0.0078 pM
IC50=4.15 pM
IC50= 3.13 pM
IFNλ1
B
B.1.617.2 (Delta)
pM IFNs